

**UKSAF Summer Meeting**  
**July 2018**

**Presentations & Young Surface Analysis (YSA)**  
**Abstract Book**



**harwellxps**

# Charge Compensation & Reduction in XPS - Friend or Foe?

David Morgan

Email: [MorganDJ3@cardiff.ac.uk](mailto:MorganDJ3@cardiff.ac.uk)

School of Chemistry, Cardiff University & HarwellXPS, The EPSRC National Facility for XPS

## Abstract

Charge neutralisation in x-ray photoelectron spectroscopy (XPS) is commonplace for the analysis of semi-conducting and insulating materials. However, the influence on surface chemistry of the materials studied is often neglected.

Herein, preliminary work is presented on a comparison of both electron and electron-ion charge compensation methods and the influence on surface chemistry of a variety of materials and discuss methods to minimise any potential changes during XPS analysis for such sensitive materials.

# Photoinduced Force Microscopy:

## A New Ambient Surface Science Technique?

### Abstract

Infrared Photo-induced Force Microscopy (IR PiFM) is based on an atomic force microscopy (AFM) platform that is coupled to a widely tunable mid-IR laser. PiFM measures the dipole induced at or near the surface of a sample by an excitation light source by detecting the dipole-dipole force that exists between the induced dipole in the sample and the mirror image dipole in the metallic AFM tip. This interaction is strongly affected by the optical absorption spectrum of the sample, thereby providing a significant spectral contrast mechanism which can be used to differentiate between chemical species. Due to its AFM heritage, PiFM acquires both the topography and spectral images concurrently and naturally provides information on the relationship between local chemistry and topology with sub 10 nm spatial resolution on a variety of samples. PiFM spectral images surpass spectral images that are generated via other techniques such as scanning transmission X-ray microscopy (based on synchrotron source), micro confocal Raman microscopy, and electron microscopes, both in spatial resolution and chemical specificity. The breadth of the capabilities of PiFM will be highlighted by presenting data on various material systems (organics, inorganics, 1D/2D, bio-molecules, and nano-photonic materials). These include high surface-sensitivity at ambient pressure. By enabling imaging at the nm-scale with chemical specificity, PiFM provides a powerful new analytical method for deepening our understanding of nanomaterials and facilitating technological applications of such materials.

### Bio

(PiFM was invented and is developed by Prof Kumar Wickramasinghe of UC Irvine and veteran AFM pioneer Dr Sung Park who founded Park Scientific Instruments and latterly jointly founded Molecular Vista to develop PiFM.) Following his PhD in electron spectroscopy Ian Holton spent 18 years designing and developing XPS, Auger, surface-science and running R&D projects and teams and then running an SEM company before founding Acutance Scientific Ltd.

Richard Chater, Department of Materials, Imperial College London

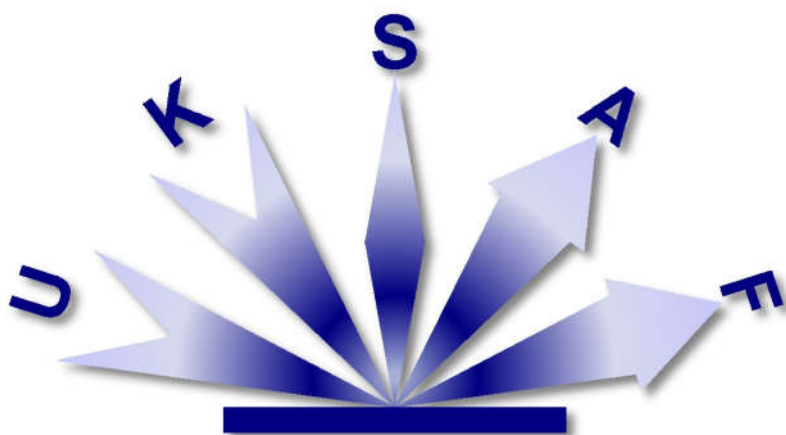
Title: Simultaneous positive and negative SIMS with ICP plasma primary ion source

Abstract: A novel UHV SIMS instrument is described based on low-field extraction of secondary ions and separate quadrupole mass spectrometers (QMS) for simultaneous positive and negative SIMS ion detection. One of the two QMS SIMS detectors can operate in both the first and second stability zones providing a high mass resolving power for +ve or –ve ions up to a mass of 20amu.

The primary ion source is a versatile inductively coupled plasma source (ICP), anchromatic mass/neutral filter and 4-lens column for a variety of source gases including oxygen, xenon and helium. Primary ion currents over a dynamic range of at least five orders of magnitude provide sputter beam for imaging, SIMS and ion beam patterning and sectioning that is an important specification for this development.

The motivation for this new SIMS instrument is described in terms of the current research programs on electrochemical devices (fuel cells, sensors, memristors and nano-channel switches) at ICL and UCL where extensive use of the labelled tracers D, Li<sup>6</sup> and O<sup>18</sup> have provided the requirement for the dual SIMS analytical finish. This instrument also includes 'in-operando' and 'pre-analysis processing' options within the vacuum envelope for introducing these labelled tracers to the samples, electrical polarisation with micro-probe contacts and heating/cooling for example with solid state lithium battery materials that are all air-sensitive.

The support from the EPSRC Strategic Equipment fund for this project is fully acknowledged. Co-investigators in this project also research projects on Alloys for Aerospace and Nuclear applications (ICL) and also with a Healthcare focus on Mineralomics (eg. <https://www.mineralomics.org/>) and Bio-medical imaging for AMD, calcification and therapeutic cancer treatments (UCL and KCL). All the thirteen co-investigators for this project have industrial partners working both national and internationally. The Project also inputs into the CDT in Materials Characterisation (ICL and UCL).



**Young Surface Analysis (YSA)**

**Abstracts**



**harwellxps**

## Elucidating the Role of Hydroxypropyl Methylcellulose in Controlling Drug Release of Pharmaceutical Tablets using Time-of-Flight Secondary Mass Spectroscopy

Pundarik, University of Nottingham

*In vitro* drug release is the standard test of tablets to predict *in vivo* release characteristics. This property depends on formulation factors and manufacturing processes used in tablet production. Hydroxypropyl methylcellulose (HPMC), a hydrophilic polymer, is frequently used for extending release in tablets. Much of the previous research about HPMC-containing tablets focuses on the effects of HPMC, such as polymer level and particle size, on release profiles. However, no scientific evidence has been provided to explain this relationship. The microstructure of HPMC particles in matrices remains unknown and might influence the ability of HPMC after contact with water to form continuous gel layers. There are relatively few contributions reporting the application of time-of-flight secondary ion mass spectrometry (ToF-SIMS) in this field, compared to other spectroscopy techniques. Regarding high surface sensitivity and a capability to generate 3D images, ToF-SIMS was applied in this study. A series of caffeine tablets containing various amounts of HPMC (7.5 - 30 %w/w) and particle size fractions (less than 45 - more than 125  $\mu\text{m}$ ) were produced and cross-sectioned using a microtomy. The tablets were subsequently analysed by ToF-SIMS and confocal Raman microscopy (CRM). Chemical maps obtained (with a focus upon HPMC) were compared and assessed using Image J. ToF-SIMS and CRM successfully distinguished key components and revealed the characteristics of compressed particles. Both results are comparable and they show that changing HPMC parameters significantly affected the tablet's microstructure. A positive linear correlation between the inter-particle distance of HPMC and the early dissolution rate of caffeine was found. This data suggests that the inter-particle distance of HPMC is indicative of its function in developing gel layers in the early dissolution periods. A significant decrease in the average particle distance was observed with increasing the HPMC content until a value of 20%, followed by a slight difference in this value found between 20 and 30% of HPMC. A possible explanation is that the HPMC content reaches a threshold where infinite HPMC particles effectively connect to each other. Decreasing particle size fractions of HPMC in the fixed HPMC content formulations resulted in the reduced inter-particle distance of HPMC, hypothetically contributing to more complete gels. The interconnectivity of HPMC networks in tablet matrices was identified using dynamic SIMS. However, future research is required to account for z-offset correction. Chemical imaging by both ToF-SIMS and CRM indicates a relationship of HPMC distribution and the dissolution rate of caffeine. These techniques, therefore, can enhance the understanding of underlying release properties and be employed in the effective formulation design and development process.

# Band alignment analysis of 2D SnS with Anatase (101), Rutile (110), and ZnO (100) by x-ray photoelectron spectroscopy.

Rosemary A. Jones<sup>1,5</sup>, David Lewis<sup>1</sup>, Karen Syres<sup>2</sup>, Aleksander A. Tedstone<sup>3</sup>, Zheshen Li<sup>4</sup>  
Paul O'Brien<sup>1,3</sup>, Andrew G. Thomas<sup>1,5</sup>.

1. School of Materials, University of Manchester, UK

2. School of Physical Sciences and Computing, University of Central Lancashire, UK

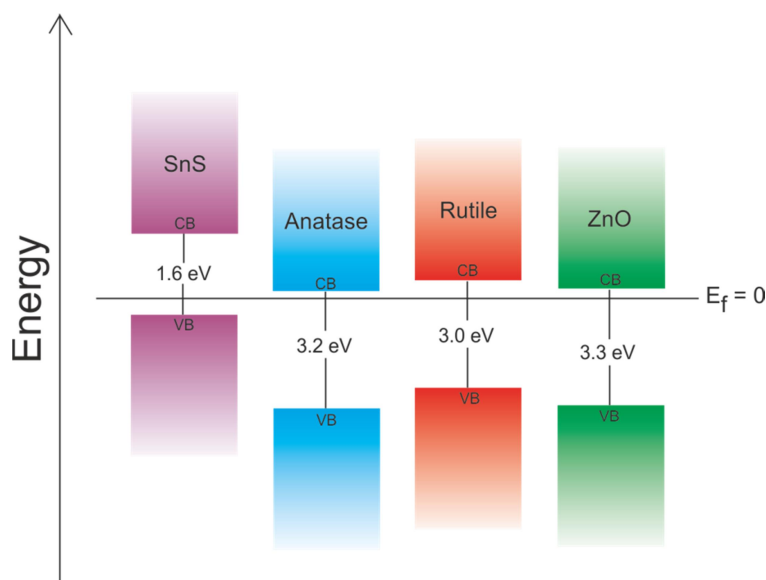
3. School of Chemistry, University of Manchester, UK

4. Department of Physics and Astronomy, Aarhus University, Denmark

5. Photon Science Institute, University of Manchester, UK

Dye, quantum dot and perovskite sensitised metal oxides are a subject of intensive research. An alternative approach to sensitising surfaces is to use small band gap 2-D materials, such as chalcogenides where the band gap can be tuned by varying the number of layers [1]. In order for such devices to operate the relative positions of valence and conduction bands of the sensitiser and n-type material is important.

Here we report on the measurement of band alignment of 2-D SnS deposited on anatase (101) surface by x-ray photoelectron spectroscopy (XPS). The 2-D SnS was obtained by liquid-phase exfoliation and deposited directly onto an anatase (101) single crystal surface, which had been cleaned under ultra-high vacuum conditions. To determine the alignment the valence band offset for the heterojunction n-TiO<sub>2</sub>/p-SnS was measured using soft XPS which gave an overlap of 0.55 eV. Literature values of the band gaps of 2-D SnS (1.6 eV) [1] and anatase TiO<sub>2</sub> (3.2 eV) [2] were used to determine the conduction band position. Analysis shows that the interface between p-SnS and single crystal anatase phase n-TiO<sub>2</sub> has a type II offset. Under the same conditions Rutile (110) and ZnO (100), with bandgaps of 3.0 eV [3] and 3.3 eV [4] respectively, also demonstrated a type II offset interface with 2-D SnS. Rutile (110) and ZnO (100) showed larger overlaps with 2-D SnS of 0.9 eV and 0.7 eV respectively.



[1.] Jack R. Brent, David J. Lewis, Tommy Lorenz, Edward A. Lewis, Nicky Savjani, Sarah J. Haigh, Gotthard Seifert, Brian Derby, and Paul O'Brien, *J. Am. Chem. Soc.*, **2015**, vol.137, issue 39, 12689–12696.

[2.] L. Kavan, M. Gräzel, J. Rathousk, and A. Zukalb, *J. Electrochem. Soc.* **1996** vol. 143, issue 2, 394-400.

[3.] B Poumellec, P J Durham and G Y Guo, *J. Phys: Condensed Matter*, **1991** vol. 3, issue 42.

[4.] S. Major, A. Banerjee, and K.L. Chopra, *Thin Solid Films*, **1983**, vol. 108, no. 3, 333–340.

# Imaging the microbe-mineral interface using high spatial resolution secondary ion mass spectrometry (NanoSIMS)

R. Lopez-Adams<sup>1</sup>, J.R. Lloyd<sup>1</sup>, K. L. Moore<sup>2</sup> and I.C. Lyon<sup>1</sup>

<sup>1</sup>School of Earth and Environmental Sciences, <sup>2</sup>School of Materials  
University of Manchester, Manchester, M13 9PL, UK.

Corresponding author ([rebeca.lopez@postgrad.manchester.ac.uk](mailto:rebeca.lopez@postgrad.manchester.ac.uk))

NanoSIMS is a surface analysis technique with high spatial resolution (down to 50 nm) and isotopic analysis capabilities which can be used to map microbial cells and the distribution of elements in their adjoining micro-environments [1, 2]. The mobility and toxicity of metals in the environment is controlled by speciation. As(III) is the most mobile and toxic form of As while As(V) is less mobile, sorbing readily to subsurface minerals, including Fe(III) oxides [3]. Arsenic contamination currently affects more than 150 million people worldwide because of its prevalence in soils and aquifers [4]. Bacteria can enzymatically oxidise or reduce arsenic (As) mobilizing or immobilising this toxic element. Some of the As reducer or oxidiser bacteria additionally reduce or oxidise Fe. However, the As(III) and Fe(II) oxidation mechanisms remain largely unclear; both direct enzymatic and indirect nitrite-mediated mechanisms have been proposed [5]. In this work we used NanoSIMS to study the active fraction of As(III)/Fe(II)-oxidiser bacteria and the key elements involved in this electron transfer process, with complimentary SEM, TEM and aqueous geochemistry.

A recently isolated As(III)-oxidiser bacteria *Acidovorax* sp. ST3 [6] was cultured in anaerobic medium amended with NaNO<sub>3</sub>, Fe(II), As(III) and <sup>13</sup>C-labelled acetate (to trace actively growing bacteria). SEM-NanoSIMS samples were prepared on silicon wafers where cells and the Fe/As precipitates were collected. The samples were analysed in a FEI Quanta 650 FEG SEM to find suitable areas prior to NanoSIMS analysis. A CAMECA NanoSIMS 50L was used with a 16 KeV Cs<sup>+</sup> primary ion beam, and aligned to detect seven masses: <sup>12</sup>C, <sup>13</sup>C, <sup>12</sup>C<sup>14</sup>N, <sup>28</sup>Si, <sup>56</sup>Fe<sup>12</sup>C, <sup>56</sup>Fe<sup>16</sup>O and <sup>75</sup>As. A FEI Tecnai F30 TEM was used to collect images and EDS spectra of samples prepared from cultures of cells grown in the same medium.

NanoSIMS analysis revealed a heterogeneous enrichment of <sup>13</sup>C labelled carbon in the cells, suggesting that not all the cells were growing and incorporating the carbon from the labelled acetate (fig 1A). This has implications in the As(III) and Fe(II) oxidation, which is mainly catalysed by active bacteria, but stored intracellular carbon could have been used in this process. There was a positive correlation between <sup>13</sup>C/<sup>12</sup>C % and As in the most active cells, implying a possible link between the metabolic rate and the amount of oxidised/precipitated As. The cell surface showed Fe encrustation (fig. 1B and C), confirmed with TEM. Fe minerals were also observed adjoining inactive cells (fig. 1A), questioning the exclusive direct role of enzymatic Fe(II) oxidation in Fe(III) mineral formation. Arsenic did not co-localise strongly with Fe in the imaged minerals in NanoSIMS, EDS in TEM revealed the presence of some As in these Fe minerals, but further mineral characterisation is needed.

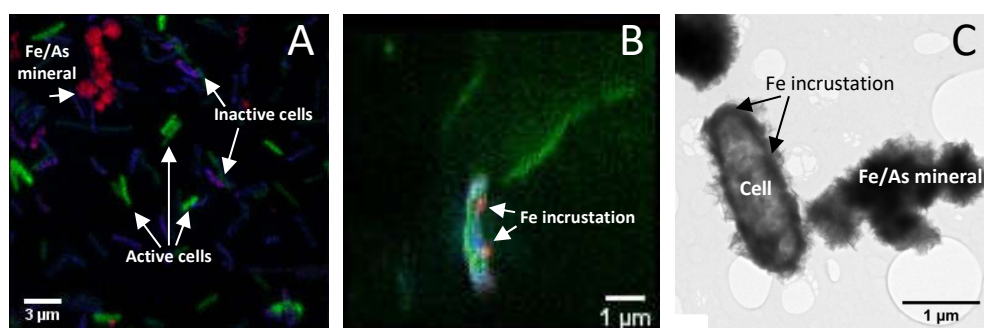


Fig. 1. NanoSIMS images (A & B), red is <sup>56</sup>Fe<sup>16</sup>O, green <sup>13</sup>C and blue <sup>75</sup>As. (C) TEM image showing Fe incrustation in the periplasm of the cell.

References: [1] Musat, N., et al. (2016) *Curr Opin Biotechnol*, 41, 114-121 [2] Gao, D., et al. (2015) *Crit Rev Biotechnol*, 8551, 1-7 [3] Zhu, Y. G., et al. (2014) *Annu Rev Earth Planet Sci*, 42, 443-467 [4] Yamamura, S. and Amachi, S. (2014) *J Biosci Bioeng*, 118, 1-9 [5] Chen, D., et al. (2018) *Chemical Geology*, 476, 59-69 [6] Zhang, J., et al. (2017) *Environ Sci Technol*, 51, 4377-4386.

## QUANTIFYING *IN VIVO* PERMEATION OF CHLORHEXIDINE DIGLUCONATE (CHG)

Khuriah Abdul Hamid, Mohammed Al-Mayahy, Nichola J. Starr, Andrew L. Hook, Maria Marlow, David J. Scurr

School of Pharmacy, University of Nottingham, NG7 2RD, Nottingham, United Kingdom

### Background:

Skin permeation and distribution of a conventional antimicrobial compound, chlorhexidine digluconate (CHG), has been successfully demonstrated using Time-of-flight secondary ion mass spectrometry (ToF-SIMS). This method is advantageous as it does not require laborious preparation, radio-labels or fluorescent tags. However, the disadvantage of this technique is that it is not inherently quantitative. This study aims to develop calibration data-sets to enable quantitative data to be derived from ToF-SIMS skin permeation analysis. This will be then related to *in vivo* data acquired for CHG permeation in human volunteers.

### Methods:

Porcine skin was homogenised, using a rotor-stator homogeniser (Ultra-Turrax) and mixed with 20% w/v CHG solutions in the concentration range of 0.039-8.75 µg/mg. These were printed using a contact printer (BIODOT) and analysed using a ToF-SIMS IV instrument (IONTOF, GmbH). In the *in vivo* study, volunteer's forearms were treated with 4% and 2% hibiscrub and 2% Chloraprep™ with samples subsequently analysed by ToF-SIMS.

### Results:

A calibration microarray of skin / CHG spots was successfully printed. Analysis by ToF-SIMS allowed the generation of a calibration curve which showed a linear correlation between CHG concentration and CHG ion intensity. An examination of CHG fragment ion images revealed that the CHG spots are uniformly printed. The ToF-SIMS analysis of the *in vivo* tape strips indicated that the samples treated with 4 % hibiscrub show an enhanced permeation as compared to the 2 % equivalent and the Chloraprep™. Furthermore, these results can be quantified using the calibration data derived from skin / CHG microarray.

### Conclusions:

A uniform skin tissue microarray was successfully printed illustrated a directly proportional relationship between CHG ion intensity and CHG concentration. This enabled the quantification of ToF-SIMS data acquired from *in vivo* testing of the permeation of CHG.

## Surface alteration evidences for a mechanism of anoxic dissolution of UO<sub>2</sub>

Aleksej J. Popel<sup>1,\*</sup>, Beng Thye Tan<sup>1</sup>, Giulio I. Lampronti<sup>1</sup>, Jason Day<sup>1</sup>, Rachel Eloirdi<sup>2</sup>,  
Thomas Gouder<sup>2</sup>, Ian Farnan<sup>1</sup>

<sup>1</sup>Department of Earth Sciences, University of Cambridge, Downing Street, Cambridge, CB2 3EQ, United Kingdom,

<sup>2</sup>European Commission, Joint Research Centre, Directorate G for Nuclear Safety and Security, Unit G.I.5, Advanced Nuclear Knowledge unit, Postfach 2340, 76215 Karlsruhe, Germany.

A secondary phase has been observed to nucleate on the surface of UO<sub>2</sub> (see Fig. 1) in a solution with uranium concentration values of  $\sim 10^{-9}$  mol/l. The UO<sub>2</sub> was in the form of a 100 nm single crystalline film epitaxially deposited on the (001) surface of a single crystalline silicon substrate. An extended (140 days) dissolution experiment with UO<sub>2</sub> in contact with a solution in deoxygenated, deionised water, under Ar atmosphere ( $\sim 0.1$  O<sub>2</sub> ppm) at ambient temperature ( $\sim 25$  °C) suggests that uranium dioxide should dissolve and re-precipitate through U<sup>4+</sup> oxidation state to enable nucleation of a low solubility secondary phase. Dissolution of U<sup>4+</sup> at defective reactive sites [1, 2] with subsequent nucleation in a less defective form has been suggested to take place during anoxic dissolution of UO<sub>2</sub> in deionised water (Eq. 1):

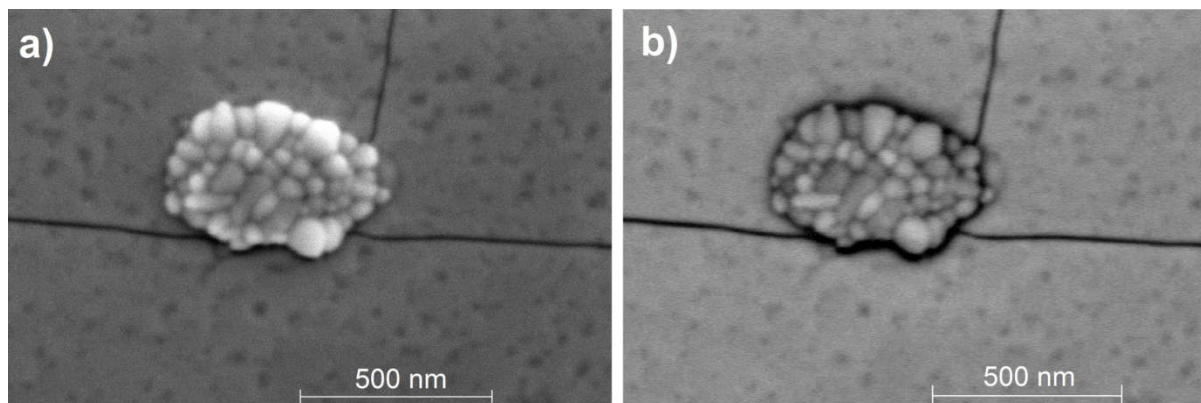
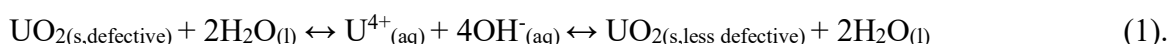


**Fig. 1.** Secondary (a) and backscatter electron (b) micrographs showing nucleated secondary phases at a junction point of the UO<sub>2</sub> film cracks.

### References

- [1] C.L. Corkhill, D.J. Bailey, F.Y. Tocino, M.C. Stennett, J.A. Miller, J.L. Provis, K.P. Travis, N.C. Hyatt, Role of Microstructure and Surface Defects on the Dissolution Kinetics of CeO<sub>2</sub>, a UO<sub>2</sub> Fuel Analogue, *ACS Appl. Mater. Interfaces* 8 (2016) 10562-10571.
- [2] C.L. Corkhill, E. Myllykyla, D.J. Bailey, S.M. Thornber, J. Qi, P. Maldonado, M.C. Stennett, A. Hamilton, N.C. Hyatt, Contribution of energetically reactive surface features to

---

\* Corresponding author e-mail: [ap499@cam.ac.uk](mailto:ap499@cam.ac.uk)

the dissolution of CeO<sub>2</sub> and ThO<sub>2</sub> analogues for spent nuclear fuel microstructures, ACS Appl. Mater. Interfaces 6 (2014) 12279-12289.

# Identifying Metabolic Heterogeneity in Mammary Gland Tumours using the 3D-OrbiSIMS.

Yulia Panina<sup>1,2</sup>, Peter Kreuzaler<sup>1</sup>, Ian Gilmore<sup>2</sup>, Mariia Yuneva<sup>1</sup>

(1) *Oncogenes and Tumour Metabolism Lab, The Francis Crick Institute, 1 Midland Road, London, NW1 1AT, UK*

(2) *National Centre of Excellence in Mass Spectrometry Imaging, National Physical Laboratory, Hampton Road, Teddington, TW11 0LW, UK*

Deregulated metabolism is a key hallmark of cancer, and is often characterised by differential metabolic enzyme and nutrient transporter expression, as well as increased or differential metabolism of key nutrients such as glucose and glutamine for energetic and anabolic functions (1). Metabolic changes contribute to well-established tumour heterogeneity, which is a major challenge for anti-cancer therapeutics (2). Visualising and quantifying the spatial distribution of metabolites and the activity of metabolic pathways within different tumour regions and different cell types composing a tumour as well as in surrounding healthy tissue can unveil metabolic vulnerabilities for novel or combination therapies.

Understanding the intra- and inter-tumour heterogeneity is a principle aim for developing therapies for tumour types where altered metabolism contributes to cancer progression. Factors contributing to metabolic reprogramming and heterogeneity in cancer include oncogene-induced signalling pathways, interaction between diverse cell populations within the tumour microenvironment and adaptation to differential nutrient availability, particularly in the context of different organ sites in metastasis (3, 4). Mammary gland tumours driven by the Myc oncogene are highly diverse in genetic, histologic and metabolic signatures and are among the most aggressive breast cancer tumours with poor patient prognosis.

In order to understand the dynamic metabolic heterogeneity in Myc-driven mammary gland tumours, we are using Secondary Ion Mass Spectrometry (SIMS) imaging, which allows analysis of both the structural architecture and chemical composition of intact tumour samples. The 3D-OrbiSIMS is a new instrument with a QExactive HF Orbitrap mass analyser that allows specific detection and mapping of metabolic ion signals *in situ* with pristine mass resolving power (240,000 at  $m/z$  200) and sub-cellular lateral resolution (2  $\mu\text{m}$ ) (5). Furthermore, the instrument is equipped with a micro-focussed argon gas cluster ion beam for gentler desorption with significantly less fragmentation compared with typical liquid metal ion beam ( $\text{Bi}^{3+}$ ) used for SIMS imaging (6). These unique detection capabilities allow accurate visualisation and identification of polar and lipid metabolites *in situ*, with the aim of understanding metabolic plasticity in the diverse, heterogeneous microenvironment of mammary gland tumours and their metastases.

1. Yuneva M. Finding an "Achilles' heel" of cancer: the role of glucose and glutamine metabolism in the survival of transformed cells. *Cell Cycle*. 2008;7(14):2083-9.
2. Robertson-Tessi M, Gillies RJ, Gatenby RA, Anderson ARA. Impact of metabolic heterogeneity on tumor growth, invasion and treatment outcomes. *Cancer Research*. 2015;75(8):1567-79.
3. Andrechek ER, Cardiff RD, Chang JT, Gatza ML, Acharya CR, Potti A, et al. Genetic heterogeneity of Myc-induced mammary tumors reflecting diverse phenotypes including metastatic potential. *Proc Natl Acad Sci U S A*. 2009;106(38):16387-92.
4. Christen S, Lorendeau D, Schmieder R, Broekaert D, Metzger K, Veys K, et al. Breast Cancer-Derived Lung Metastases Show Increased Pyruvate Carboxylase-Dependent Anaplerosis. *Cell Rep*. 2016;17(3):837-48.
5. Passarelli MK, Pirkel A, Moellers R, Grinfeld D, Kollmer F, Havelund R, et al. The 3D OrbiSIMS-label-free metabolic imaging with subcellular lateral resolution and high mass-resolving power. *Nat Methods*. 2017;14(12):1175-83.
6. Havelund R, Pirkel A, Passarelli M, Newman CF, Moellers R, Arlinghaus H, et al. Label-free Imaging of Biomolecules in Murine Brain Sections Using the 3D OrbiSIMS. In: NiCE-MSI N, editor. *Nature Protocol Exchange* 2017.

### 3D OrbiSIMS imaging of *Drosophila* cuticular lipids

Clare L. Newell<sup>1,2</sup>, Ian S. Gilmore<sup>2</sup>, Alex P. Gould<sup>1</sup>

<sup>1</sup> The Francis Crick Institute, 1 Midland Road, London, NW1 1AT, UK

<sup>2</sup> National Centre for Excellence in Mass Spectrometry Imaging (NiCE MSI), National Physical Laboratory, Hampton Road, Teddington, TW11 0LW, UK

The body surface (cuticle) of the fruit fly *Drosophila melanogaster* is coated in a complex blend of lipids which perform a variety of functions including protection against water-loss and pheromonal communication. This blend is composed of a variety of different lipid classes including hydrocarbons, wax esters and fatty acids. Many previous studies have focused on hydrocarbons <sup>1</sup> but little is known about the other components. Here, we demonstrate that 3D OrbiSIMS can be used to analyse individual wax esters and other lipids on the cuticle in a way that has thus far not been possible using more traditional mass spectrometry. 3D OrbiSIMS differs from other SIMS instruments as it utilises an argon GCIB primary ion beam combined with an Orbitrap mass analyser<sup>2</sup>. This instrument can achieve high spatial resolution (< 2 µm) and low compound fragmentation with the GCIB, combined with the high mass resolution (240k) and high mass accuracy (< 1 ppm) of the Orbitrap. Using these capabilities, it is now possible to image intact biomolecules with a combined high spatial and mass resolution. These advances, together with MS/MS to increase the confidence of peak assignments, now make it possible to image intact lipids in biological samples with an unprecedented level of chemical and spatial precision. This new technology reveals a surprising and hitherto unknown aspect of *Drosophila* biology - namely that wax esters and other non-hydrocarbon lipids are localised in restricted spatial patterns on the body surface. Combining 3D OrbiSIMS MS/MS with the powerful genetics of *Drosophila* now opens up, for the first time, the possibility of identifying the biosynthetic pathways for non-hydrocarbon cuticular lipids.

1. Kaftan, F. *et al.* Mass spectrometry imaging of surface lipids on intact *Drosophila melanogaster* flies. *J. Mass Spectrom.* **49**, 223–232 (2014).
2. Passarelli, M. K. *et al.* The 3D OrbiSIMS — label-free metabolic imaging with subcellular lateral resolution and high mass-resolving power. *Nat. Methods* **14**, 1175–1183 (2017).

## **The trouble with hydrogen: NanoSIMS analysis of hydrogen distribution in corroded zirconium alloys.**

*Christopher Jones<sup>1</sup>, Samuel Armson<sup>1</sup>, Michael Preuss<sup>1</sup>, Katie L. Moore<sup>1,2</sup>*

<sup>1</sup> *School of Materials, University of Manchester, Manchester, M13 9PL, UK.*

<sup>2</sup> *Photon Science Institute, University of Manchester, M13 9PL, UK*

The impact of hydrogen on the performance of zirconium alloys is an area of major concern worldwide. Zirconium alloys of various types are very widely used as structural and fuel cladding materials in several types of nuclear reactors, typically these components are critical for the safe operation of the reactor<sup>1</sup>.

Surface analysis methods, such as SIMS, are vital to understanding these materials and how they degrade in service. Using the capabilities of the NanoSIMS, mainly light element detection and high spatial resolution, along with complementary techniques, it is possible to examine the distribution of hydrogen directly, on microstructurally relevant length scales.

In this work the distribution of hydrogen in corroding zirconium alloys has been investigated and particular attention has been paid to how this distribution is affected by the damage induced by the SIMS analysis.

Two Zircaloy-2 and two Zircaloy-4 samples were corroded in autoclaves at 350°C, in simulated nuclear reactor coolant and conditions, before being transferred to static autoclaves spiked with deuterated water. Using deuterium allows unambiguous identification of hydrogen introduced during the experiment, rather than hydrogen from the sample preparation or the vacuum system. Figure 1 shows that the deuterium distribution is not uniform but it instead segregates to small particles in the zirconium metal. Through further NanoSIMS analysis and high-resolution energy dispersive X-ray spectroscopy it was found that the hydrogen segregates to Fe and Cr rich secondary phase particles.

Cr and Fe rich intermetallic particles in Zircaloys can form a Laves phase structure, these structures are known to trap hydrogen in tetrahedral interstices, with maximum capacity of up to 3.5 hydrogen atoms per molecule<sup>2</sup>.

Repeatedly imaging the same region with the Cs<sup>+</sup> ion beam, results in the distribution of the hydrogen changing dramatically, as can be seen in Figure 2(a-c). SRIM calculations identified an accumulation of sub-surface damage during analysis, which results in amorphisation of the second phase particles, destroying any trapping sites and freeing hydrogen to the  $\alpha$ -zirconium lattice. This was then confirmed by further NanoSIMS analysis and TEM imaging of the crystal structure of the secondary phase particles damaged by the NanoSIMS.

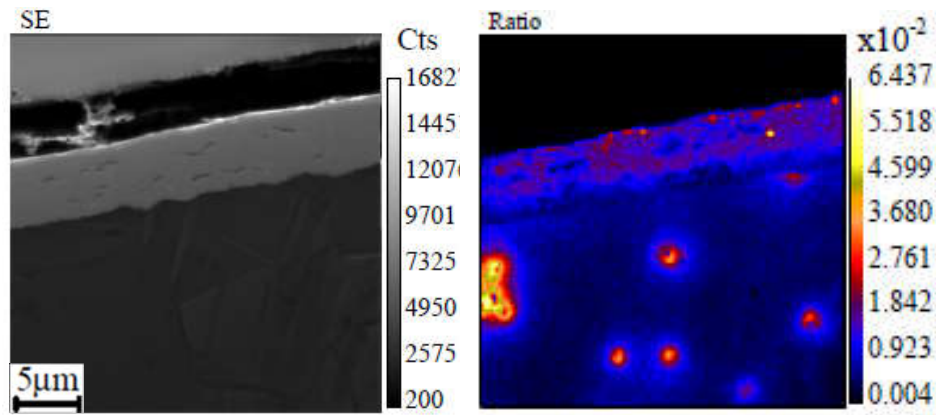


Figure 1, Secondary Electron and  $^2\text{H}/^1\text{H}$  ratio images in a Zircaloy-4 sample, in the ratio image it is clear that the hydrogen clusters around small particles in the  $\alpha$ -Zirconium lattice.

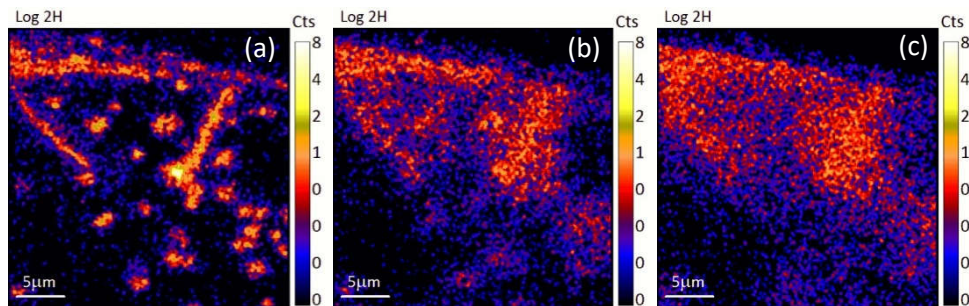


Figure 2(a-c)  $^2\text{H}$  distribution in Zircaloy-2 samples after (a) 1, (b) 8 and (c) 16 planes of NanoSIMS analysis showing the effect of ion beam damage.

1. Allen, T. R., Konings, R. J. M. & Motta, a. T. Corrosion of Zirconium Alloys. in *Comprehensive Nuclear Materials* **5**, 49–68 (Elsevier Inc., 2012).
2. Jacob, I., Shaltiel, D., Davidov, D. & Miloslavski, I. A Phenomenological Model for the Hydrogen Absorption Capacity in Pseudobinary Laves Phase Compounds. *Solid State Commun.* **23**, 669–672 (1977).

# Detecting localised deuterium in austenitic stainless steels using NanoSIMS

Yasser Al Aboura<sup>1</sup>, Anthony Cook<sup>1</sup>, Laura Felisari<sup>2</sup>, Robert Akid<sup>1</sup>, Katie L. Moore<sup>1,3</sup>

<sup>1</sup>*School of Materials, University of Manchester, Oxford Road, Manchester M13 9PL*

<sup>2</sup>*BP Formulated Products Technology, BP Technology Centre, Pangbourne, UK*

<sup>3</sup>*Photon Science Institute, University of Manchester, Oxford Road, Manchester M13 9PL*

Hydrogen damage in high strength metals can be reduced by engineering the microstructure so that hydrogen can be irreversibly trapped locally at preferential sites, thus preventing its diffusion within the lattice, in particular, to sites where cracks can initiate. Typical trap sites include second phase particles, phase interfaces and grain boundaries, each having different trapping capabilities. Analytically, it is very challenging to spatially distinguish between the different trap sites and their capacity to trap hydrogen; mainly due to the resolution and sensitivity limitations imposed by conventional characterisation techniques. The NanoSIMS is a high-resolution secondary ion mass spectrometry technique capable of spatially resolving hydrogen and its isotope deuterium thus revealing any hydrogen/deuterium enriched features.

In this study, type 303 stainless steel specimens were electrochemically charged with deuterium. Deuterium was used to minimise the effect of experimental artefacts on NanoSIMS data, notably surface adsorption of residual hydrogen present in the analysis vacuum chamber. Following charging, samples were left to outgas for 10 days in ambient conditions to allow diffusible deuterium (lattice and reversibly trapped) to effuse from the matrix, leaving behind only the irreversible trapped deuterium in the microstructure.

Deuterium enriched regions in 303 stainless steel were detected via NanoSIMS, in particular trapped deuterium associated with deformation features. The limitations of this technique are discussed, being primarily associated with the destructive nature of the ion beam during image acquisition, which leads to surface damage and topography effects. Secondary electron microscopy (SEM) and its techniques were used as complimentary tools to validate the observations.

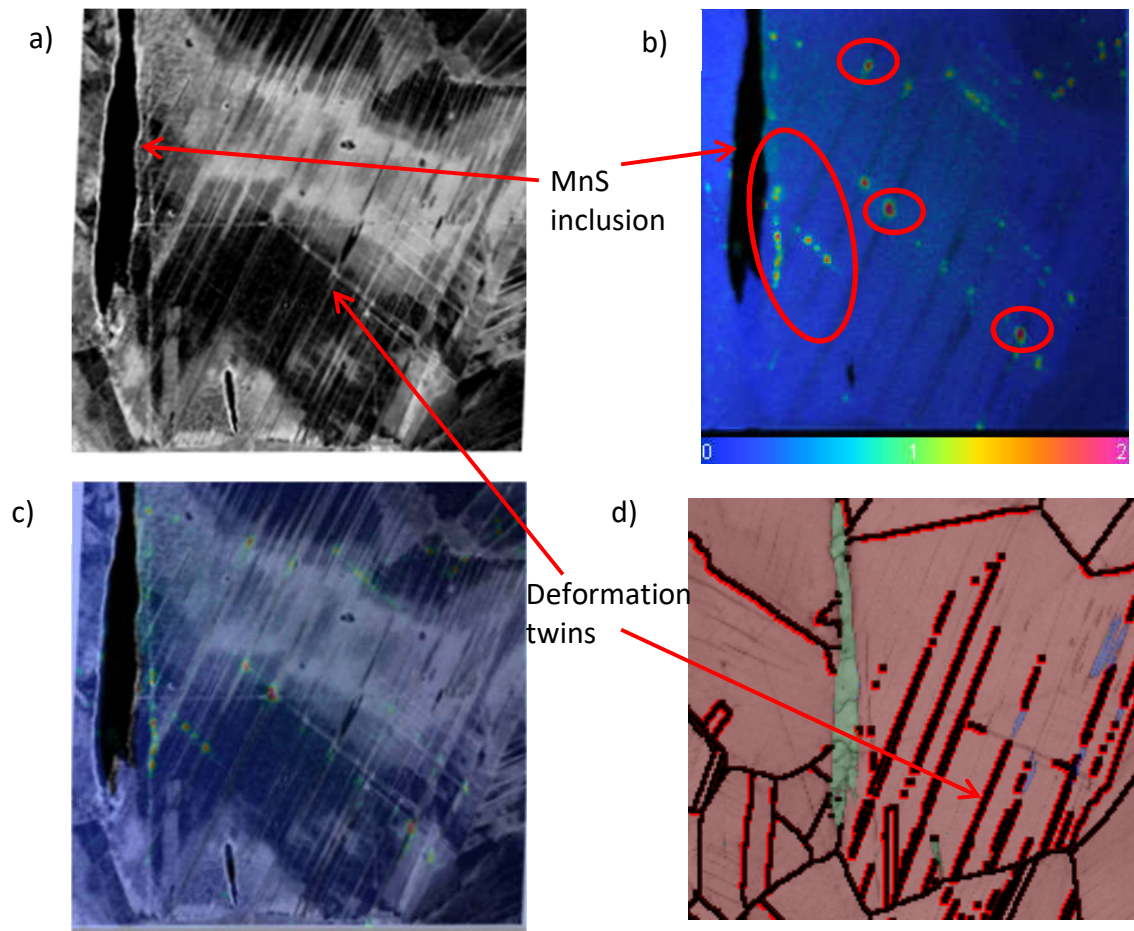


Figure 1 SEM and NanoSIMS images of a 303 stainless steel alloy highlighting a region of interest with deuterium enrichments identified at the intersection of deformation twins and shear bands (red circles). a) SEM backscatter electron map showing the deformed microstructure of the alloy. b) NanoSIMS  $^2\text{H}/^1\text{H}$  ratio map of the same region of interest in (a). c) NanoSIMS  $^2\text{H}/^1\text{H}$  ratio map overlaid over the SEM backscatter image in (a). EBSD phase map of the same region of interest; blue: BCC-ferrite, red: FCC-austenite and green: Manganese sulphide inclusion (MnS).